Available online at www.sciencedirect.com

ScienceDirect

Procedia Technology 15 (2014) 369 – 375

Procedia Technology

2nd International Conference on System-Integrated Intelligence: Challenges for Product and Production Engineering

24 GHz RFID communication system for product lifecycle applications

Johannes Meyer, Quang Huy Dao*, Bernd Geck

Institut für Hochfrequenztechnik und Funksysteme, Leibniz Universität Hannover, Appelstaße 9a, 30167 Hannover, Germany

Abstract

This paper presents the fundamental construction of a 24 GHz Radio Frequency Identification system using an optically powered transponder integrable in metal. Hereby, the system consists of a reader and a transponder. An overview of the transponder design including the modulator and demodulator circuit and its main characteristic values is given. On transponder side the communication is controlled by a low-power microcontroller. An I^2C bus is implemented allowing a flexible connection of sensors and memory. Furthermore, the reader concept is presented and a communication example is used to explain the implemented protocol.

Peer-review under responsibility of the Organizing Committee of SysInt 2014.

Keywords: RFID; optical power supply; transponder; reader; K-band

1. Introduction

Improvement of manufacturing processes and component properties are constant drivers of research in production engineering. In this context cyber-physical systems start to play an important role in production and logistics. For the identification, reproduction and the optimization of components, it is desirable to save the whole production process parameters and loads during lifecycle of each component intrinsically. Thus, the fusion between

* Corresponding author. Tel.: +49-511-762-4112; fax: +49-511-762-4010.
E-mail address: dao@hft.uni-hannover.de

Peer-review under responsibility of the Organizing Committee of SysInt 2014.
doi:10.1016/j.protcy.2014.09.091

product-related information and the product itself can be achieved. An external database to store the component and production data is not required. At the beginning of the components lifecycle, during the fabrication process the machine tools need to know which settings are best suited for each unique workpiece. This relevant information is intrinsically stored within each component and can be used to adjust individual production steps e.g. drilling, milling, and polishing. Furthermore, the vision is to give the product an opportunity to collect data via user-defined integrated sensors over its lifecycle. The recorded data can be readout at any time or during periodic inspections. This information can be used to optimize next generation of the product.

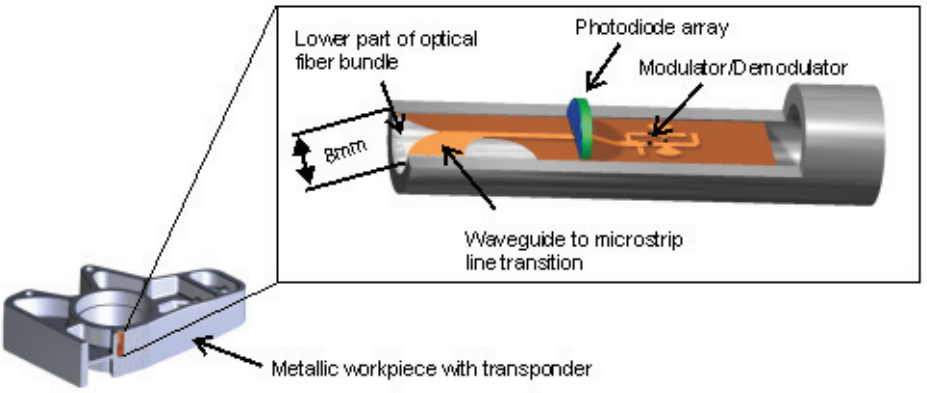

Fig. 1. 24 GHz transponder with partially removed housing (upper part of the optical fibre bundle and digital circuit are not shown).

A technology which is able to fulfill the aforementioned challenges is Radio Frequency Identification (RFID). Hereby RFID applications and the Internet of Things in general have gained a lot of attention in science and industry. RFID systems consist of a reader and a transponder, commonly referred to as tag. The field of applications is growing rapidly and it includes supply chain management, inventory control, security management, and logistics [1]. An interesting scenario for RFID systems is production engineering e.g. machine tool monitoring which is characterized by its harsh operating conditions and furthermore by a metallic environment which leads to performance degradation for many antenna concepts [2]. Thus, only specific antenna designs are suitable for an application on/in metallic objects. Commercial RFID systems operating at low frequency have a reading range of only a few millimeters [3]. In the majority of cases, UHF tags are not capable of providing sensors and large memory [4]. Most tag antenna concepts in this field are based on patch antennas that promise an excellent performance as long as they are placed on the surface of the components [5]. These kinds of solutions are an excellent choice since the operating conditions are well defined. But often transponders that are placed on the outside of the object of interest are not suitable as they can be easily destroyed by scratching them off. Hence, transponder concepts that are integrable into metallic objects are necessary. An approach that addresses the aforementioned challenges is presented in this contribution. This procedure utilizes a new transponder type that is completely integrated in a drill hole which serves as a circular aperture antenna on the surface of the metallic workpiece. Furthermore, the drill hole is used as waveguide with an integrated inline waveguide to microstrip transition. The transition is necessary for the integration and the connection of the RF and digital components of the transponder. Hence, the sensitive electronic components of the tag are protected from the environment. The range of applications is mainly determined by the geometrical volume of the transponder as it mechanically weakens the metallic components. Thus, a minimization of the transponder – which is basically determined by the circular waveguide – is desirable. For this reason the 24 GHz Industrial, Scientific and Medical band (ISM) is used for the practical implementation of the transponder since the required drill size diameter is inversely proportional to the carrier frequency. The high frequency leads to large free space attenuation. Hence, a passive tag concept powered by the microwave field of the reader is not suitable. Thus, RFID hybrid systems [6], [7] that combine microwave data communication and optical power supply are used in this paper to overcome the power supply limitations. Fig. 1

shows the optically power supplied transponder in detail and gives an impression of the integration in a metallic wheel carrier.

2. Optically power supplied transponder applicable in metal

The block diagram of the RFID system presented in this contribution is shown in Fig. 2a. Hereby, the reader is illustrated on the left side and the optically power supplied transponder is depicted on the right side. A brief summary of the transponder and its characteristic values is given in the following. As shown in Fig. 1 the transponder can be divided into the main parts: antenna with integrated photodiode array, modulator/demodulator and digital circuit which is not visible as it is positioned at the back of the substrate material opposite to the analog circuit. Both, analog and digital circuits share the same ground plane which is placed between the two substrates. The aperture antenna is realized by a dielectrically loaded circular waveguide with a diameter of 8 mm. It features a broad radiation characteristic with a halfpower beamwidth of approximately 70° and a measured gain of 4.4 dBi. For optimal optical power supply two bundles of polymer optical fibers separated by the waveguide to microstrip line transition are inserted in the waveguide. In Fig. 1 only the lower bundle is shown. The fibers guide the incident light to the photodiodes. Both bundles have a half circular cross section. The combination of the light source and the photodiode array has to deliver a peak power supply of approximately 3.6 mW to power up the digital circuit of the transponder. The photodiode array consists of six photodiode segments that are connected in series to provide at least 2 V which is necessary to guarantee the functionality of the digital components. The diameter of the single fiber within the bundle is optimized to obtain an even light distribution on the photodiode array and it is chosen to 1 mm [8]. Furthermore, a waveguide to microstrip transition is inserted between the polymer optical fiber bundles, allowing the connection of the modulator and demodulator circuit which is also referred to as analog frontend. A detailed description of the antenna concept combining optical power supply and microwave data reception is presented in [9]. The design of the analog frontend will be discussed in the following section.

2.1. Modulator and Demodulator

For a bi-directional communication with the reader, the tag requires a modulator and demodulator which are positioned behind the photodiode array to minimize shading (cf. Fig. 1). The concept for this analog frontend is based on a preliminary study [10] and will be described in the following. The layout of the optimized frontend is shown in Fig. 2b. Hereby, the marked area in the lower part and the highlighted area in the upper part represent the demodulator and the modulator, respectively.

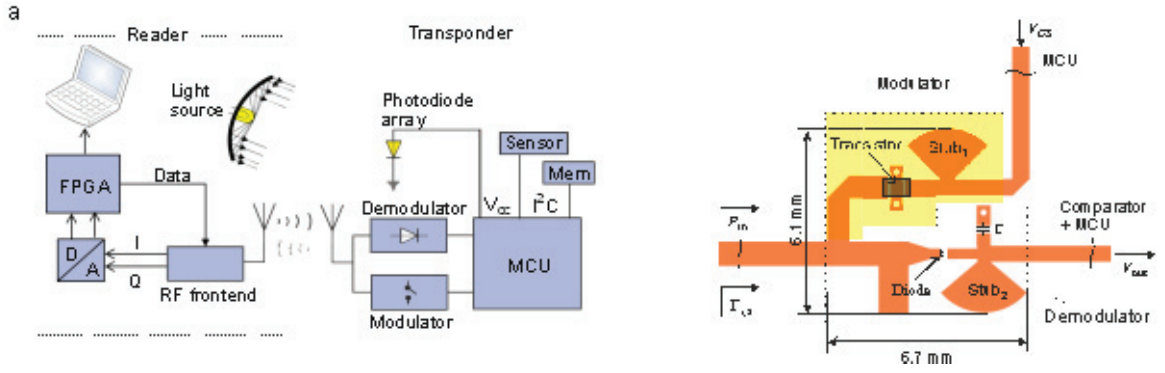

Fig. 2. (a) Block diagram of the RFID system, (b) layout of the realized analogue frontend.

The modulator is based on an Avago VMMK-1225 High Electron Mobility Transistor (HEMT) which is placed at the antenna feed point in a shunt configuration. Hence, the backscattering method is used to realize an on-off keying to transmit information from the transponder to the reader. Hereby, the transistor provides two different

reflection coefficients at the antenna feed point which are necessary for the backscattering method [11]. As the two input reflection coefficients $\Gamma_{1,2}$ are defined by the gate source voltage of the transistor, data can be transferred to the reader by changing this voltage according to the applied data. Consequently, the gate of the HEMT is connected to a Microcontroller Unit (MCU). Furthermore, the usage of a HEMT offers low power consumption (3.7 µW @ V_{GS} = 0.7 V) and good backscatter performance. Hence, a power efficient communication from the transponder to the reader is obtained.

The comparison between measurement and simulation of the two resulting reflection states Γ_1 and Γ_2 is depicted in Fig. 3a. They are characterized for a frequency range of 20-26 GHz and the used 24 GHz ISM band is highlighted in grey. As a transistor is a nonlinear device the reflection coefficients have to be determined as a function of the applied incident power. For the sake of clarity the comparison is only shown for -20 dBm input power. Hereby, Γ_1 represents the matched case and Γ_2 the mismatched case which are obtained for a gate source voltage of 0 V and 0.7 V, respectively. The simulation results of the high frequency circuit were attained by Agilent Advanced Design System 2009 (ADS). For the determination of the measured reflection coefficients a setup based on a vector network analyzer was used. The comparison between the simulated and measured results shows an excellent agreement. The measured magnitude of the two states can be accomplished to $|\Gamma_1|$ = -15 dB and $|\Gamma_2|$ = -2 dB at an input power of -20 dBm for the operating frequency.

The demodulator unit is realized by an envelope detector which consists of a high performance Schottky diode (Agilent HSCH-9161) and a microwave 0.3 pF capacitor. Thus, the request from the reader based on Amplitude Shift Keying (ASK) can be demodulated. The optimized demodulator performance was also obtained using ADS. An enveloped demodulator is mainly characterized by its voltage sensitivity which also determines the communication distance of this RFID system as explained later. The characterization of the sensitivity is a function of the incident power and frequency as the behavior of Schottky diodes is influenced by them. Therefore, a signal generator with adjustable source power and operation frequency is connected to the input of the analog frontend and the converted direct current signal is detected at the output of the demodulator. The resulting three-dimensional representation of the measured output voltage V_{out} as a function of the incident power P_{in} and the operation frequency f is illustrated in Fig. 3b. For the application within the transponder the output signal of the demodulator has to be applied to a comparator which shifts the signal to the logic level of the MCU. Hence, the threshold voltage of the comparator defines the voltage sensitivity of the transponder. According to the measurement results the sensitivity is -29 dBm at center frequency. The realized analog frontend has the dimensions of 6.7 x 6.1 mm, thus fitting into the drill hole.

Both the modulator and demodulator are controlled by a TI MSP430 F2013 microcontroller as it offers very low power consumption. Furthermore, the digital circuitry of the transponder implements an I^2C bus, thus, allowing a flexible connection of sensors and memory. The digital components are placed on a separate layer to minimize the overall volume of the transponder which is of essential interest. Hence, the combination of the three aforementioned main parts of the transponder (antenna, analog frontend, digital circuit) lead to a three layered printed circuit board (PCB) with the dimensions of 8 mm in width, 26 mm in length and 0.5 mm in height. In the following section a description of the reader and an exemplary communication between reader and transponder are presented.

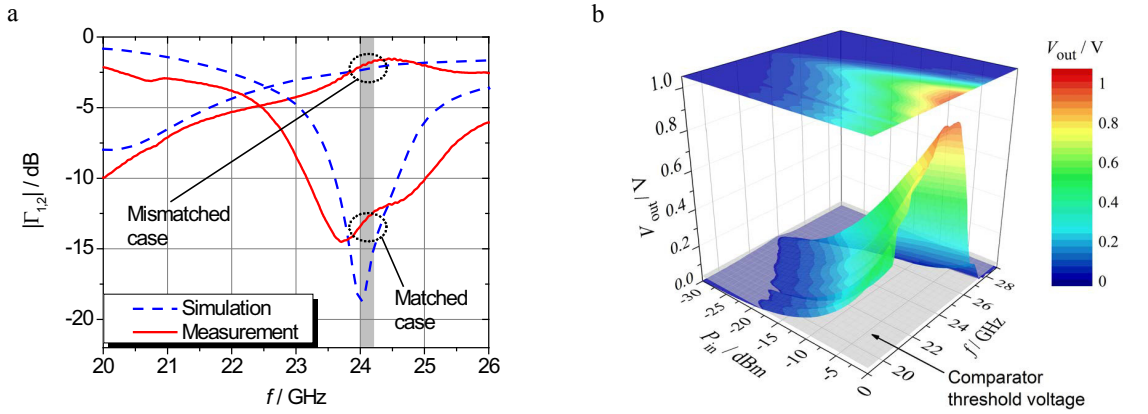

Fig. 3. (a) Comparison between simulated and measured reflection coefficient for the matched and mismatched case; (b) Measured voltage at the output of the analog frontend.

3. System evaluation

The reader is realized in a monostatic configuration based on plug-in devices. The reader hardware can be divided into the analog and the digital unit, the light source and the antenna. The segmentation allows a flexible adaption to changes or future developments within the RFID system. The microwave source of the reader and the antenna are adjusted to 20 dBm (EIRP) output power which are imposed by mandatory regulations for the 24 GHz ISM band. On the reader side the ASK modulation is accomplished by a PIN diode switch which is controlled by the digital unit of the reader, allowing an on-off keying as a function of the applied data. The received backscattered data from the transponder are demodulated utilizing a homodyne receiver based on an I/Q mixer followed by a high pass and a low frequency amplifier. The digital unit is placed in a separate case and consists of a Field-Programmable Gate Array (FPGA) and two A/D converters. The FPGA decodes and encodes the data according to the communication protocol described later. Finally, a MATLAB graphical user interface is implemented to transfer raw data or requests from a PC to the FPGA and vice versa. A measurement setup including the reader and the transponder inserted into a wheel carrier is depicted in Fig. 4a. The communication distance of the described RFID system can be estimate by the modified Friis equation [12]:

$$d = \sqrt{\frac{G_{\mathrm{Reader}} \cdot P_{\mathrm{Reader}} \cdot G_{Tag} \cdot \lambda_0^2}{(4 \cdot \pi)^2 \cdot P_{Tag}} \left(1 - |\Gamma_1|^2\right)} \tag{1}$$

where the product of G_{Reader} P_{Reader} is limited by mandatory regulation for the 24 GHz ISM band, G_{Tag} is the gain of the transponder antenna, P_{Tag} is the received power of the tag, λ_0 is the free space wavelength and Γ_1 is the reflection coefficient as mentioned before. Thus, the maximum communication distance is determined by $|\Gamma_1|^2$ which is almost zero and P_{Tag} which equals the sensitivity of the demodulator. As a result the theoretical distance amounts to d = 0.47 m. This communication distance is also verified by a measurement. The data rate in both directions is 80 kbit/s but it can be theoretically increased to 400 kbit/s by adjusting the clock of the MCU. This would lead to a significantly increased power demand, though. The resulted power consumption of the transponder is so efficient that it can work even under bright sun light conditions.

A communication example (request for current temperature value) between the reader and the transponder is shown in Fig. 4b. The measured signal is recorded at the baseband output ports of the reader. For the sake of

visibility only the inphase channel is shown. The signal includes the request from the reader which occurs within the first 270 µs. Due to the processing time of the transponder MCU the response of the transponder has a delay of approximately 3.1 ms. The implemented protocol can be divided into three sections that are shown in the lower part of Fig. 4b: preamble, data and checksum. The line coding used for the communication is a Manchester code [13]. Hereby, a logical one is represented as a rising slope and a zero is represented by a falling slope. The preamble is mainly used for time recovery and it determines the beginning of the data stream. The start condition is realized by three consecutively followed logical states with the same value which is not valid for Manchester coding. The data string follows the preamble. Furthermore, a higher level data protocol has been implemented to allow sequencing multiple packets as required by operations such as reading from or writing to the integrated 8 kB EEPROM. Finally, a checksum is used to detect errors on the wireless link. As mentioned before the backscattered transponder response is converted into the baseband and this signal is processed by a FPGA that decodes the data. Finally, a graphical user interface allows the user to display received demodulated data e.g. current temperature value.

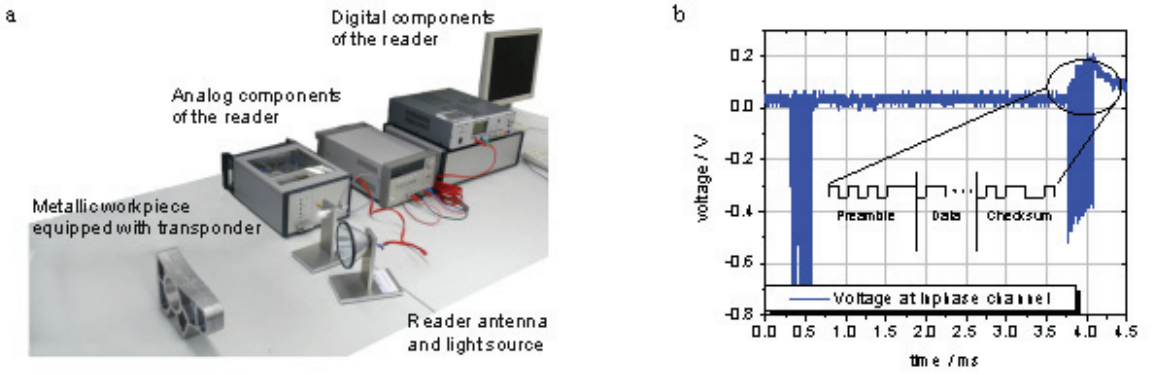

Fig. 4. (a) Setup of the RFID system with reader and transponder integrated into wheel carrier; (b) communication flow of a reader request for the current temperature sensor value and the response of the transponder.

4. Conclusion

This paper presents a RFID system working in the 24 GHz ISM band. The key features of the system are the optical power supply of the transponder and its ability to be applicable in metal. The whole transponder dimensions are 26 mm in length and 8 mm in diameter. The realized analog frontend consists of only three high frequency discrete components in order to accomplish the task of modulation and demodulation. Due to the microcontroller based transponder design and the modular design of the reader the system is extremely flexible. Sensors can be easily added to the transponder due to the I^2C bus. The construction of the system components reader and transponder and the communication protocol are discussed. Due to the high efficiency of the transponder a power supply by bright sunlight is sufficient for a simple communication between transponder and reader. In this case an external light source is not needed. A future development is a RFID system which will work under indoor lighting conditions. The system supports a communication distance of 0.5 m and a data rate of 80 kbit/s.

Acknowledgements

The authors wish to thank the German Research Foundation for the financial support in the framework of the Collaborative Research Center 653. Furthermore, the authors wish to thank Mr. Bernard Lüers and Mr. Christopher Seifert for help implementing the data protocol.

References

[1] Finkenzeller K. RFID Handbook. 2nd ed. Hoboken, New Jersey: John Wiley & Sons; 2004.
[2] Dobkin D, Weigand S. Environmental effects on RFID tag antennas. In: Microwave Symposium Digest, 2005 IEEE MTT-S International; 2005.
[3] NeoTAG Inlay MF2626. Neosid; 2012; www.neosid.de.
[4] Embeddable Tags. Xerafy; 2013; www.xerafy.com.
[5] Kim JS, Choi W, Choi GY. UHF RFID tag antenna using two PIFAs embedded in metallic objects. Electronics Letters 2008;44(20):1181–1182.
[6] Turpin T, Baktur R. Meshed patch antennas integrated on solar cells, Antennas and Wireless Propagation Letters. IEEE 2009;(8):693–696.
[7] Caso R, D'Alessandro A, Michel A, and Nepa P. Integration of slot antennas in commercial photovoltaic panels for stand-alone communication systems. IEEE Transactions on Antennas and Propagation 2013;61(1):62–69.
[8] Franke S, Meyer J, Overmeyer L. Hybrid waveguides for energy transmission by light and RF communication in metal components. In: Smart Systems Integration; 2011.
[9] Meyer J, Franke S, Geck B, and Overmeyer L. Hybrid antenna design for an optically powered SHF RFID transponder applicable in metals. International Journal of Microwave and Wireless Technologies 2013, invited.
[10] Meyer J, Dao QH, Geck B. Design of a 24 GHz analog frontend for an optically powered RFID transponder for the integration into metallic components. In: 43rd European Microwave Conference (EuMC) 2013.
[11] Dobkin DM. The RF in RFID. Passive UHF RFIF in Practice. Oxford: Newnes; 2007.
[12] Nikitin PV, Rao KVS, Martinez RD. Differential RCS of RFID tag. Electronics Letters 2007;(43):431–432.
[13] Lehpamer H. RFID Design Principles. London: Artech House; 2008.